One-Loop Effects in Supergravity Models with an Additional U(1)

D.A. Demir, N. K. Pak
Middle East Technical University, Department of Physics, 06531, Ankara, Turkey
(February 1, 2008)

Abstract

For an Abelian extended Supergravity model, we investigate some important low energy parameters: $\tan\beta$, $Z-Z'$ mixing angle, lightest CP-even Higgs mass bound, Z' mass, and effective μ parameter. By integrating the RGE's from string scale down to the weak scale we constuct the scalar potential, and analyze the quantities above at the tree- and one-loop levels by including the contributions of top squarks and top quark in the effective potential.
PACS: 04.65.+e, 12.60.Jv

I. INTRODUCTION

There are several reasons for considering additional $U(1)$ symmetries and their associated extra Z bosons. Such additional $U(1)$'s arise after the breaking of GUT's (for example $E(6)$-based rank-5 models), or in string compactifications. In addition to justifying the underlying model, more importantly, additional $U(1)$'s would also solve the MSSM μ problem when broken around the weak scale. Indeed, as was already argued in [1], in a large class of string models, breaking scale of the extra $U(1)$'s come out to be below a TeV.

The phenomenologically viable models should satisfy two conditions at the string scale: Firstly, the extra $U(1)$ should be non-anomalous and should not acquire a mass from the string or hidden sector dynamics; namely, its mass must come from the gauge symmetry breaking in the observable sector. Secondly, all scalar soft mass-squareds must be positive and of similar magnitude. The latter holds in gravity-mediated SUSY breaking scheme, where the mass scale is given by the gravitino mass, not necessarily, so however, in gauge-mediated SUSY breaking schemes.

Soft terms, parametrizing our ignorance of the origin of the SUSY breaking, can be obtained from a general supergravity (SUGRA) Lagrangian in $M_{Pl} \to \infty$ limit [2,3]. Although, the minimal SUGRA predicts universal soft terms, in general SUGRA theories (see [4] and references therein), and in superstring theories [5] it is possible to have non-universal soft terms. Thus, considering such explicit examples, one is free to consider non-universal boundary conditions [6], without referring to the particular case of universality.

For testing such extra $U(1)$ models in near-future machines, the tree-level potential is clearly not sufficient; one has to take into account the radiative corrections to have a meaningful model at these energies. Among other methods [7], the effective potential approach proved to be an elegant and simple way of icorporating the radiative corrections to the scalar potential [8,9], which we will adopt in this work as well.

This work is organized as foollows: In Sec. 2 we shall first describe the model at the SUGRA scale. Using one loop RGE's we shall obtain all the low energy potential parameters as functions of their SUGRA scale values. After discussing the requirements on the low energy potential for phenomenological viablility, we determine the appropriate SUGRA scale parameter space. We do this with minimal amount of non-universality. That is, we allow for non-universality only between Higgs doublets and remaining scalars; in particular, we choose doublet soft mass-squareds to be equal and one order of magnitude smaller than the others.

In Sec. 3 we consider the issue of radiative corrections. Out of all fields which can contribute to the effective potential, we consider top quark and stops contributions, and neglect the remaining fields. We assume that the log effects which are accounted for in solving the RGE's, are enough to take into account the effects of Higgs, neutralino, chargino, and vector boson loops, at least for calculating the low-lying mass spectrum [10].

In Sec. 4 we work out the one-loop potential numerically, and graph the tree- and one-loop results together to enable a comparative discussion of the effects of the radiative corrections.

In Sec. 5 we discuss the results of the work in the light of near-future accelerators, and MSSM and NMSSM predictions.

II. LOW-ENERGY TREE-LEVEL POTENTIAL

As is well known, the fundamental SUGRA scale $M = M_{Pl}/\sqrt{8\pi}$ is approximately one order of magnitude larger than the MSSM coupling constant unification level $M_U \approx 10^{16}\, GeV$ [11]. However, the threshold effects [13,14] can close the gap, and thus, in the following we shall choose the MSSM unification scale M_U as the starting point of the analysis at which the initial conditions of the potential parameters are specified. We reconsider a general, anomaly-free, Abelian extended SUSY model which was discussed in [12] already. The model is specified by an Abelian extension of the MSSM gauge group: $G = SU(3)_c \times SU(2) \times U(1)_Y \times U(1)_{Y'}$ with the couplings g_3, g_2, g_Y, $g_{Y'}$, respectively. The particle content for one family is given by the left-handed chiral superfields: $\hat{L} \sim (1, 2, -1/2, Q'_L)$, $\hat{E}^c \sim (1, 1, 1, Q'_E)$, $\hat{Q} \sim (3, 2, 1/6, Q'_Q)$, $\hat{U}^c \sim (\bar{3}, 1, -2/3, Q'_U)$, $\hat{D}^c \sim (\bar{3}, 1, 1/3, Q'_D)$. The Higgs sector contains the $SU(2)$ doublets $\hat{H}_1 \sim (1, 2, -1/2, Q'_1)$ and $\hat{H}_2 \sim (1, 2, 1/2, Q'_2)$, and the SM-singlet $\hat{S} \sim (1, 1, 0, Q'_S)$.

The superpotential for the model is given by

$$f = h_s^0\, \hat{S}\hat{H}_1.\hat{H}_2 + h_t^0\, \hat{U}^c\hat{Q}.\hat{H}_2 \tag{1}$$

where the family mixings are ignored. We kept only the top and Higgs Yukawa couplings, as the Yukawa coupings of the other fermions are much smaller.The existence of $U(1)_{Y'}$ group makes the model totally different from NMSSM by forbidding an elementary μ term and an S^3 term (so that the superpotential does not have a Z_3 symmetry).

Without specializing to a particular class of string compactifications, we parameterize the supersymmetry breaking by considering the most general soft supersymmetry breaking terms:

$$\begin{aligned} V_{SOFT} = \; & = m_1^{0\,2} \mid H_1 \mid^2 + m_2^{0\,2} \mid H_2 \mid^2 + m_S^{0\,2} \mid S \mid^2 + m_U^{0\,2} \mid \tilde{t}_L^c \mid^2 \\ & + m_Q^{0\,2} \mid \tilde{Q} \mid^2 - h_s^0 A_s^0 (S H_1.H_2 + h.c.) - h_t^0 A_t^0 (\tilde{t}_L^{c*} \tilde{Q}.H_2 + h.c.) \\ & + \sum_a M_a^0 \lambda^a \lambda^a . \end{aligned} \tag{2}$$

Here λ^a are gauginos with the masses M_a^0, and $\tilde{t}_L^c$ and $\tilde{Q}$ are the scalar components of $\hat{U}^c$ and $\hat{Q}$, respectively. The superscript nought on each quantity designates its value at the SUGRA scale which is determined by the VEV's of the hidden sector fields (moduli and dilaton fields, in the case of string compactifications), modulo the threshold corrections.

The scalar components of the Higgs superfields are assigned the following representation under $SU(2)$ group:

$$\hat{H}_1 \longrightarrow H_1 = \begin{pmatrix} H_1^0 \\ H_1^- \end{pmatrix} \;,\; \hat{H}_2 \longrightarrow H_2 = \begin{pmatrix} H_2^+ \\ H_2^0 \end{pmatrix} \;,\; \hat{S} \longrightarrow S \,. \tag{3}$$

Adding to V_{SOFT} the usual F-term and D-terms of the associated group factors, one obtains the full scalar potential, whose Higgs part reads

$$\begin{aligned} V_0 = & \, m_1^{0\,2} \mid H_1 \mid^2 + m_2^{0\,2} \mid H_2 \mid^2 + m_S^{0\,2} \mid S \mid^2 + \lambda_1^0 \mid H_1 \mid^4 + \lambda_2^0 \mid H_2 \mid^4 \\ & + \lambda_S^0 \mid S \mid^4 + \lambda_{12}^0 \mid H_1 \mid^2 \mid H_2 \mid^2 + \lambda_{1S}^0 \mid H_1 \mid^2 \mid S \mid^2 + \lambda_{2S}^0 \mid H_2 \mid^2 \mid S \mid^2 \\ & - h_s^0 A_s^0 (S H_1.H_2 + h.c.)\} \end{aligned} \tag{4}$$

The terms involving parameters λ_i^0 come from the supersymmetric part of the Lagrangian consisting of F and D terms, and their explicit expressions are listed below:

$$\begin{aligned}
\lambda_1^0 &= \frac{1}{8}G_0^2 + \frac{1}{2}{g_{Y'}^0}^2 {Q'}_1^2 \\
\lambda_2^0 &= \frac{1}{8}G_0^2 + \frac{1}{2}{g_{Y'}^0}^2 {Q'}_2^2 \\
\lambda_S^0 &= \frac{1}{2}{g_{Y'}^0}^2 {Q'}_2^2 \\
\lambda_{12}^0 &= -\frac{1}{4}G_0^2 + {g_{Y'}^0}^2 {Q'}_1 {Q'}_2 + h_s^{0\,2} \\
\lambda_{1S}^0 &= {g_{Y'}^0}^2 {Q'}_1 {Q'}_S + h_s^{0\,2} \\
\lambda_{2S}^0 &= {g_{Y'}^0}^2 {Q'}_2 {Q'}_S + h_s^{0\,2}
\end{aligned} \tag{5}$$

where $G^0 = \sqrt{{g_2^0}^2 + {g_Y^0}^2}$. As there is no experimental constraint on $U(1)_{Y'}$ group, $g_{Y'}$ is arbitrary. However, for realistic models it is expected that $g_{1'} \sim g_1$ [15], so we assume the unification of $g_{1'}$ with the other gauge couplings at the the MSSM unification scale M_U [11]. Using the trace formulas for the fermion sector

$$\begin{aligned}
Tr[Q_{color}^2] = Tr[Q_{isospin}^2] = 2\,,\; Tr[Y^2] = \frac{10}{3}\,, \\
Tr[Y'^2] = 6{Q'}_Q^2 + 3({Q'}_U^2 + {Q'}_D^2) + 2{Q'}_L^2 + {Q'}_E^2
\end{aligned} \tag{6}$$

we normalize the gauge couplings such that, at M_U, they satisfy

$$g_3^0 = g_2^0 = g_1^0 = g_{1'}^0 = g^0\ , \tag{7}$$

with the normalized $U(1)_Y$ and $U(1)_{Y'}$ couplings,

$$g_1^0 = \sqrt{\frac{5}{3}} g_Y^0\ ,\ g_{1'}^0 = \sqrt{\frac{6{Q'}_Q^2 + 3({Q'}_U^2 + {Q'}_D^2) + 2{Q'}_L^2 + {Q'}_E^2}{2}}\, g_{Y'}^0\ . \tag{8}$$

In obtaining the renormalization group flow of the parameters of the potential we shall consider one-loop RGE's which were listed in Appendix A of [12]. We assume that the scale of SUSY breaking is around the weak scale, and thus we integrate RGE's of a softly broken SUSY model from the SUGRA scale down to the weak scale directly. Among the RGE's the most complicated ones are those involving Yukawa couplings h_s and h_t which obey coupled nonlinear equations. The top Yukawa coupling h_t reaches its fixed point value of $h_t \sim 1-1.2$ almost independently of the initial conditions h_s^0 and h_t^0. Corresponding to this h_s takes values around $0.6 - 0.8$. On the other hand, the RGE's of soft masses, being linear, can be solved exactly as a function of their initial conditions, for given h_s^0 and h_t^0. Finally, as a by-product of the coupling constant unification, it is natural to assume a common mass $M_{1/2}$ for all gauginos at the SUGRA scale.

In constructing the solutions of RGE's one needs to specify the $U(1)_{Y'}$ charges of the fields. Without referring to specific $E(6)$ based charge assignments, one can relate different $U(1)_{Y'}$ charges to each other by imposing the cancellation of the triangular anomalies together with the gauge invariance of the potential. The superpotential in (1) includes only

the top and Higgs trilinear mass terms, and thus we shall require the gauge invariance for these vertices only, leaving other the would-be vertices (such as $\hat{E}^c\hat{L}.\hat{H}_1$) unconstrained. Then the solution of $U(1)_{Y'}$ charges reads

$$\begin{aligned} &Q'_S = -(Q'_1 + Q'_2)\ ,\ Q'_U = (Q'_1 - 3Q'_2)/3\ ,\ Q'_D = (Q'_1 + 3Q'_2)/3\,, \\ &Q'_E = -(Q'_1 - Q'_2)\ ,\ Q'_Q = -Q'_1/3\ ,\ Q'_L = -Q'_2, \end{aligned} \tag{9}$$

which fix all but the two (Q'_1 and Q'_2) of the $U(1)_{Y'}$ charges. The advantageous side of this solution set is that it leaves the $U(1)_{Y'}$ charges of Higgs doublets free, which will be important in analyzing the mixing angle of Z boson and $U(1)_{Y'}$ gauge boson. We give this solution for the third family, and assume vanishing $U(1)_{Y'}$ charges for the first two families. This is allowed in non-geometrical string compactifications (such as free-fermionic models), where a given Higgs doublet couples only one family [16]. As will be discussed later on, third family coupling of $U(1)_{Y'}$ is important in analyzing the Z' models with LEP constraints. Finally, for future use, we make the choice $Q'_1 = Q'_2 = -1$ in (9) which fix all of the $U(1)_{Y'}$ charges. Then, the solution of RGE's, with the initial values $h_s^0 = h_t^0 = \sqrt{2}g^0$ for Yukawa couplings, read as follows:

$$\begin{aligned} h_s &= 0.595 \\ h_t &= 1.028 \\ A_s &= 0.42A_s^0 - 0.272A_t^0 - 0.285M_{1/2} \\ A_t &= -0.045A_s^0 + 0.128A_t^0 + 1.755M_{1/2} \\ m_1^2 &= -0.064A_s^{0\,2} + 0.036A_s^0A_t^0 + 0.007A_t^{0\,2} - 0.01A_s^0M_{1/2} + 0.019A_t^0M_{1/2} \\ &\quad + 0.52M_{1/2}^2 + 0.047(m_Q^{0\,2} + m_U^{0\,2}) - 0.16m_S^{0\,2} + 0.84m_1^{0\,2} - 0.11m_2^{0\,2} \\ m_2^2 &= -0.038A_s^{0\,2} + 0.037A_s^0A_t^0 - 0.048A_t^{0\,2} + 0.045A_s^0M_{1/2} - 0.19A_t^0M_{1/2} \\ &\quad - 2.47M_{1/2}^2 - 0.41(m_Q^{0\,2} + m_U^{0\,2}) - 0.1m_S^{0\,2} - 0.1m_1^{0\,2} + 0.485m_2^{0\,2} \\ m_S^2 &= -0.128A_s^{0\,2} + 0.072A_s^0A_t^0 + 0.014A_t^{0\,2} - 0.021A_s^0M_{1/2} + 0.039A_t^0M_{1/2} \\ &\quad + 0.081M_{1/2}^2 + 0.094(m_Q^{0\,2} + m_U^{0\,2}) + 0.68m_S^{0\,2} - 0.32m_1^{0\,2} - 0.22m_2^{0\,2} \\ m_U^2 &= 0.017A_s^{0\,2} + 0.0005A_s^0A_t^0 - 0.037A_t^{0\,2} + 0.037A_s^0M_{1/2} - 0.139A_t^0M_{1/2} \\ &\quad + 3.27M_{1/2}^2 - 0.306m_Q^{0\,2} + 0.69m_U^{0\,2} + 0.038m_S^{0\,2} + 0.038m_1^{0\,2} - 0.27m_2^{0\,2} \\ m_Q^2 &= 0.009A_s^{0\,2} + 0.0002A_s^0A_t^0 - 0.018A_t^{0\,2} + 0.019A_s^0M_{1/2} - 0.07A_t^0M_{1/2} \\ &\quad + 4.72M_{1/2}^2 + 0.85m_Q^{0\,2} - 0.15m_U^{0\,2} + 0.02m_S^{0\,2} + 0.02m_1^{0\,2} - 0.13m_2^{0\,2} \end{aligned} \tag{10}$$

As a result of the normalization of the gauge couplings the low energy parameters are not very sensitive to the assignmets of the $U(1)_{Y'}$ charges. For example, if one chooses a model with $E(6)$ charge assignments, the results are affected only by a few percents. Thus, from a practical point of view, one can regard the above-listed solutions as independent of $U(1)_{Y'}$ charge assignments. On the contrary, dependence of the low energy parameters, especially the triliear couplings, on the variations of the initial conditions of Yukawa couplings is important. In what follows we shall confine ourselves to $h_s^0 = h_t^0 = \sqrt{2}g^0$ [16], as was already used in obtaining (10). The low energy potential with the parameters in (10) is a

general one, and thus one has to specify the appropriate region of the parameter space to satisfy the phenomenological requirements existing at the weak scale.

After the breaking of gauge symmetry down to $SU(3)_c \times U(1)_{em}$, there will arise two neutral massive gauge bosons Z and Z' whose mass matrix reads

$$(\mathcal{M}^2)_{Z-Z'} = \begin{pmatrix} M_Z^2 & \Delta^2 \\ \Delta^2 & M_{Z'}^2 \end{pmatrix}, \tag{11}$$

where

$$M_Z^2 = \frac{1}{4} G^2 (v_1^2 + v_2^2), \tag{12}$$

$$M_{Z'}^2 = g_{Y'}^2 (v_1^2 Q_1^2 + v_2^2 Q_2^2 + v_s^2 Q_S^2), \tag{13}$$

$$\Delta^2 = \frac{1}{2} g_{Y'}\, G (v_1^2 Q_1 - v_2^2 Q_2), \tag{14}$$

and, Higgs VEV's are defined as

$$< H_1^0 >= v_1/\sqrt{2}\ ;\ < H_2^0 >= v_2/\sqrt{2}\ ;\ < S^0 >= v_s/\sqrt{2}. \tag{15}$$

There are three main conditions that the vacuum state must satisfy:

- The W boson mass must remain at its LEP1 value, as the model is exteded only in the neutral direction,
- The color and charge symmetries must remain unbroken,
- The $Z - Z'$ mixing angle α must be below $a\ few\ \times 10^{-3}$ as otherwise the LEPI value of M_Z is destructed.

The first condition can be satisfied using the fact that the potential (4) has a common mass scale defined by the gravitino mass, as the soft SUSY breaking terms in (2) are generated by the SUGRA breaking. Thus, the mass scale of the potential, m_0 (proportional to the gravitino mass), can be factored out and remaining dimensionless potential can be minimized freely. The first condition above can then be met by imposing the constraint

$$m_0 \sqrt{f_1^2 + f_2^2} = 246\, GeV \tag{16}$$

where f_1 and f_2 are the dimensionless H_1 and H_2 VEV's, which are defined as $v_1 = m_0 f_1, v_2 = m_0 f_2$, and for future use $v_s = m_0 f_s$.

The charge breaking can arise from both Higgs and squark sectors. In the Higgs sector, with the help of $SU(2)$ symmetry, a possible $< H_2^+ >$ can be rotated away, and the charge breaking can be parametrised in terms of $v_- =< H_1^- >$. As can be calculated easily, the potential prefers the charge preserving minimum, if $\tilde{A} > 0$, where

$$\tilde{A} = 2 \sin^2\beta\, m_{H^\pm}^2, \tag{17}$$

$\tan\beta = v_2/v_1$, and $m_{H^\pm}^2$ is the charged Higgs boson mass-squared. Consequently, in what follows we shall work in that portion of the parameter space where the charged Higgs boson has real mass, so that the charge breaking in the Higgs sector is avoided.

When, at least one of $< \tilde{t}_L^c >$, $< \tilde{Q} >$, take a nonzero value, both color and charge symmetries are broken. To prevent the formation of such a minimum, one has to have a certain hierarcy between the top trilinear coupling A_t and the soft squark mass parameters. In fact, the usual criterium [17] $h_t^2 A_t^2 < 3(m_Q^2 + m_U^2 + m_2^2)$ must hold at a scale $Q \sim A_t/h_t$. More importantly, when the squark masses go negative, a charge and/or color breaking minimum will be developed, even if it is secondary. When analyzing the low energy potential, we shall always keep these conditions in mind.

That the $Z - Z'$ mixing angle is to be small is a severe constraint on the vacuum state. The $Z - Z'$ mixing angle, α, is generated by the off-diagonal elements of the $Z - Z'$ mass matrix (10), and given by

$$\alpha = \frac{1}{2} \arctan \left(\frac{2\Delta^2}{M_{Z'}^2 - M_Z^2} \right) \tag{18}$$

There are mainly three regions of parameter space of the pure Higgs sector yielding a small α:

1. *Heavy Z' Minimum* : As is seen from (18), when $M_{Z'} >> M_Z$, α becomes small. This occurs in that portion of the parameter space satisfying,

$$-m_S^2 >> |m_1^2|\,,\, |m_2^2|\,,\, (h_s A_s)^2 \tag{19}$$

for which Higgs VEV's behave like

$$v_s \sim \sqrt{-m_S^2/\lambda_s} >> v_1\,,\, v_2. \tag{20}$$

This ordering of the VEV's make Δ^2 small compared to $M_{Z'}^2$, whereby producing a small mixing angle. This mechanism does not require any relationship among the soft masses m_1^2 and m_2^2, and charges Q_1' and Q_2'; it utilizes only the ordering in (19). $\tan\beta$, however, is closely related to the values of charges Q_1', Q_2' and the values of the soft masses m_1^2 and m_2^2. When $-m_S^2$ takes higher and higher values, only $U(1)_{Y'}$ gets broken, and other group factors remain unbroken. This introduces a mass scale $Q = \sqrt{-m_S^2}$ between weak and SUGRA scales; remnants of the gauge group must be broken by a second stage around the weak scale. Before the occurance of such an intermediate scale, large $-m_S^2$ can create a relatively large μ parameter, thus $-m_S^2$ getting large values must be avoided.

2. *Light Z' Minimum* : As (18) suggests, another way of obtaining a small mixing angle would be to make Δ^2 small irrespective of the value of $M_{Z'}$. To obtain this kind of cancellation, one needs roughly $v_1^2/v_2^2 \sim |Q_2'/Q_1'|$ which may be satisfied in some limited portion of the parameter space. However, unlike MSSM and like NMSSM, the existence of the trilinear coupling parameter $h_S A_s$ opens a new avenue in obtaining an appropriate electroweak breaking. That is, when

$$h_S^2 A_s^2 >> |m_1^2|, |m_2^2|, |m_S^2| \tag{21}$$

holds, all VEV's are drawn approximately to the same point:

$$v_1 \sim v_2 \sim v_s \sim A_s/(h_S\sqrt{2}). \tag{22}$$

If the $U(1)_{Y'}$ charges of Higgs doublets satisfy $Q'_2 = Q'_1$, this large trilinear coupling-induced minimum cancels $Z - Z'$ mixing, allowing M_Z to be compatible with LEPI data. Such a light Z' must show up in the Z-pole observables, and therefore parameters of the model can be constrained using LEP1 data. As a side remark, the passage of the trilinear coupling from lower values to higher ones (compared to the soft masses) is either a first order or second order phase transition, depending on the sign of $m^2 = m_1^2 + m_2^2 + m_S^2$. In fact, if m^2 is positive, there is a first order phase transition occuring at the critical point $A_s^{crit} = \sqrt{8\,m^2/3}$.

3. *Hybrid Minimum* : One can obtain a phenomenologically viable minimum in all aspects by combining the parameter spaces of *Heavy Z′ Minimum* and *Light Z′ Minimum*. To do this, one can choose both $-m_S^2$ and A_s^2 large compared to other soft masses. As large A_s^2 pushes all Higgs VEV's to the same point, and $-m_S^2$ prefers a large SM-singlet VEV, when both $-m_S^2$ and A_s^2 are large, doublet VEV's (controlled by A_s via (22)) will approach to approximately the same value, and SM-singlet VEV (controlled by $-m_S^2$ via (20)) will be much larger than them. Thus, this portion of the parameter space yields a small mixing angle together with a relatively heavy Z'. In the analyses below, we shall be mainly interested in this kind of parameter space and assume $Q'_1 = Q'_2$. Actually, when $-m_S^2$ is large, one does not need this condition, as Δ^2 in (14) is already small compared to $M_{Z'}^2$. However, this kind of choice allows for the realization of the required minimum in a reasonable range of parameter values.

In the above- mentioned low- energy analysis we have required a certain hierarchy among the potential parameters. However, as dictated by the solution of RGE's in (10), it is not realistic to consider such idealized cases since as one parameter changes, all others do too as a function of the initial conditions. Moreover, we need not only the Higgs sector parameters, bu also the parameters of the squark sector as we shall calculate the 1-loop squark contributions to the Higgs potential. Thus, one has to determine the SUGRA scale parameter space consistently by considering all the low energy parameters simultaneously.

Once non-universality is permitted, one faces with a huge parameter space each point of which corresponds to some symmetry breaking scheme at low energies. The usual procedure for the determination of the appropriate portion of the parameter space, would be to trace the SUGRA-scale parmeter space point-by-point, and pick up those yielding a viable minimum at low energies. However, with the low energy parameters in (10), and the constraints implied by the *Hybrid Minimum*, we can determine the appropriate parameter space analytically. In accordance with the conditions coming from the *Hybrid Mininum*, we want to speed up $-m_S^2$ and A_s compared to other mass parameters in terms of their dependence on a choosen SUGRA scale parameter. These two have three parameters, A_s^0, A_t^0 and $M_{1/2}$, in common, and we shall use A_s^0 as a probe for determining the appropriate parameter space, by fixing other parameters with minimal amount of non-universality [6]. To slow down the A_s^0 dependence of m_1^2 and m_2^2, we make the following choice for $m_1^{0\,2}$ and $m_2^{0\,2}$:

$$m_1^{0\,2} \approx m_2^{0\,2} \approx A_s^{0\,2}/10 \tag{23}$$

For the remaining parameters we keep universality:

$$m_S^{0\,2} = m_Q^{0\,2} = m_U^{0\,2} = A_t^{0\,2}/3, \tag{24}$$

and finally we let $M_{1/2} = A_t^0$. Under these conditions, the low energy parameters read as follows:

$$\begin{aligned}
A_s &\approx 0.42\, A_s^0 - 0.58\, A_t^0 \\
A_t &\approx -0.045\, A_s^0 + 1.9\, A_t^0 \\
m_1^2 &\approx 0.026\, A_s^0 A_t^0 + 0.53\, A_t^{0\,2} \\
m_2^2 &\approx 0.08\, A_s^0 A_t^0 - 3.5\, A_t^{0\,2} \\
m_S^2 &\approx -0.18\, A_s^{0\,2} + 0.05\, A_s^0 A_t^0 + 0.43\, A_t^{0\,2} \\
m_Q^2 &\approx -0.0026\, A_s^{0\,2} + 0.02\, A_s^0 A_t^0 + 5.0\, A_t^{0\,2} \\
m_U^2 &\approx -0.0052\, A_s^{0\,2} + 0.04\, A_s^0 A_t^0 + 3.4\, A_t^{0\,2}
\end{aligned} \tag{25}$$

As we see from these equations the quadratic $A_s^{0\,2}$ dependence of m_1^2 and m_2^2 are supressed compared to those of the others with m_S^2 being the fastest one among all concerning their $A_s^{0\,2}$ dependence. In the analysis below we shall vary

$$\zeta = A_s^0/A_t^0 \tag{26}$$

in a certain range of values, and determine A_t^0 from the invariance of the $W^\pm$ mass under such Abelian extensions of MSSM. When ζ is small, except for m_2^2, all soft masses are positive, yielding a non-zero f_2 and vanishing f_1, f_2. This is not an acceptable minimum, as the gauge symmetry is not broken completely. As ζ increases, m_2^2 starts overcoming the large negative threshold coming from (essentially the $SU(3)_c$) gaugino masses, and H_1^0 and S do develop nonzero VEV's. But still it may not yield a small enough mixing angle. Further increase of ζ brings us to the sought minimum where $0 \neq f_1 \sim f_2 << f_s$. However, this increase cannot be maintained further as the squark masses turn to negative after overcoming their large positive mass thresholds dominated by the $SU(3)_c$ gaugino. Negative squark masses cause charge and color breaking minima, even if secondary, so that this limiting case will be avoided below.

III. ONE-LOOP CORRECTIONS

Until now our discussion has been based solely on the RGE-improved tree-level potential. However, quantum corrections beyond the log effects included in the RGE analysis are important. Especially the top-stop sector gives the most important contribution due to the relatively large value of top Yukawa coupling. To take such radiative corrections into account we shall follow efective potential approach [8,9] in which the radiatively corrected one-loop potential is given by

$$V_1 = V + \Delta V \tag{27}$$

where the one-loop contribution has the Coleman-Weinberg form

$$\Delta V = \frac{1}{64\pi^2} Str\mathcal{M}^4 \ln \frac{\mathcal{M}^2}{Q^2} \ , \tag{28}$$

where Str is the usual supertrace and $\mathcal{M}^2$ is the field dependent mass-squared matrix. We have transferred a renormalization scheme dependent constant into a redefinition of the renormalization scale Q^2. One notes that all the parameters in (27) are to be evaluated at the scale $Q^2 \sim \mathcal{O}(v_1^2 + v_2^2)$. Indeed, this is consistent with the RGE analysis of the last section as we have integrated them from the SUGRA scale down to the weak scale. In the loop expression (28) we consider only the contributions of top and stops $\tilde{t}_2$, $\tilde{t}_1$ whose masses are given by

$$m_t = h_t |H_2^0| \ ; \ m^2_{\tilde{t}_{1,2}} = \frac{1}{2}\{m_{11}^2 + m_{22}^2 \pm \sqrt{(m_{11} - m_{22})^2 + 4|m_{12}|^2}\} \tag{29}$$

where

$$\begin{aligned} m_{11} &= m_Q^2 + \lambda_{1t}|H_1|^2 + \lambda_{2t}|H_2|^2 + \lambda_{st}|S|^2 + \tilde{\lambda}_{1Q}|H_1^0|^2 + \tilde{\lambda}_{2Q}|H_2^+|^2 \\ m_{22} &= m_U^2 + \lambda_{1u}|H_1|^2 + \lambda_{2u}|H_2|^2 + \lambda_{su}|S|^2 \\ m_{12} &= -h_t A_t H_2^{0*} + h_s h_t S^* H_1^{0*} \end{aligned} \tag{30}$$

and the dimensionless coefficients

$$\begin{aligned} \lambda_{1t} &= -g_2^2/4 - g_Y^2/12 + g_{Y'}^2 Q'_1 Q'_Q \\ \lambda_{2t} &= -g_2^2/4 - g_Y^2/12 + g_{Y'}^2 Q'_2 Q'_Q + h_t^2 \\ \lambda_{st} &= g_{Y'}^2 Q'_S Q'_Q \\ \lambda_{1u} &= g_{Y'}^2 Q'_1 Q'_U \\ \lambda_{2u} &= g_{Y'}^2 Q'_2 Q'_U + h_t^2 \\ \lambda_{su} &= g_{Y'}^2 Q'_S Q'_U \\ \tilde{\lambda}_{1Q} &= g_2^2/2 \\ \tilde{\lambda}_{2Q} &= g_2^2/2 - h_t^2 \end{aligned} \tag{31}$$

follow from the colored sector of the full scalar potential. We shall calculate radiative corrections to the lightest CP-even Higgs mass bound, so we are interested in the CP-even scalar mass-squared matrix which can be obtained by evaluating $\frac{\partial^2 V_1}{\partial\phi_i \partial\phi_j}$ at the VEV's, in the basis $(Re[H_1^0], Re[H_1^0], Re[S^0])$.

Before going into a detailed numerical analysis, we first present a general discussion on the effects of the radiative corrections based on some approximate formulae. The top-stop splitting $S_{t\tilde{t}} = \ln \frac{m_{\tilde{t}_1} m_{\tilde{t}_2}}{m_t^2}$ and stop splitting $S_{\tilde{t}\tilde{t}} = m^2_{\tilde{t}_1} - m^2_{\tilde{t}_2}$ describe the most important contributions of the one-loop corrections. On the other hand, due to the choice of Q^2, the remaining log $\ln \frac{m_t^2}{Q^2}$ is not as important as the former ones. To extract some information about the effects of the loop corrections on the tree level parameters, one can expand the minimization equations in powers of stop splitting and identify the renormalization effects

on the tree-level quantities. In fact, to lowest order in stop splitting $S_{\tilde{t}\tilde{t}}$, and neglecting the terms involving the gauge couplings, one finds that the most important contributions come to A_s, m_2^2 and λ_2; which are given by

$$\begin{aligned}\hat{A}_s &= A_s + \beta_{h_t} S_{t\tilde{t}} A_t \\ \hat{m}_2^2 &= m_2^2 + \beta_{h_t}[(A^2 + A_t^2) S_{t\tilde{t}} - A^2] \\ \hat{\lambda}_2 &= \lambda_2 + \beta_{h_t} S_{t\tilde{t}} h_t^2\end{aligned} \tag{32}$$

where $\beta_{h_t} = \frac{3}{(4\pi)^2} h_t^2$, and $A^2 = m_Q^2 + m_U^2$. Let us now discuss the implications of these one-loop corrections in the light of the RGE solution set in (25). As the first equation in (32) shows, A_s is strengthened by the loop corrections. However, A_s^0 dependence of A_t is approximately one order of magnitude smaller than that of A_s so that one does not have a significant improvment for A_s, unless top-stop splitting is large. The improvement in m_2^2, $\delta m_2^2 \sim \beta_{h_t} A^2 (S_{t\tilde{t}} - 1)$ depends, in addition to A^2 itself, on how large $S_{t\tilde{t}}$ is compared to unity. That is, if the stop masses are large compared to m_t, the top-stop splitting can be large enough to give a significant contribution to m_2^2. Hence, both A_s and m_2^2 get significantly improved if the top-stop splitting is large enough. As one can read off from (25), for small ζ, the squark soft masses are large due to the contribution of the $SU(3)_c$ gaugino. Therefore, m_2^2 is significantly improved by the loop corrections in this range of the ζ values. However, we observe from (25) that for larger ζ values A^2 gets smaller and the loop contributions drop significantly. Finally, as dictated by (32), H_2 quartic coupling λ_2 is significantly improved by the radiative corrections if the top-stop splitting is large enough. In the small ζ limit, one has $f_2 \sim \sqrt{-m_2^2/\lambda_2} >> f_1, f_s$, which clearly shows that tree-level f_2 is larger than the loop-level one. This radiative reduction in f_2 causes one-loop $\tan\beta$ to drop:

$$\tan^2\hat{\beta} = \tan^2\beta (1 - \tan\beta \, \frac{\beta_{h_t}[(A^2 + A_t^2 + 2m_t^2) S_{t\tilde{t}} - A^2]}{A_s \mu_s}) \tag{33}$$

where the effective MSSM μ parameter $\mu_s = (h_s v_s)/\sqrt{2}$ is introduced. Indeed, with the contributions of $\hat{m}_2^2$ and $\hat{\lambda}_2$, one-loop $\tan\beta$ is reduced compared to the tree-level one. However, the inverse $\mu_s A_s$ dependence will force the loop contribution to drop rapidly after some ζ values. In this sense, one expects tree- and loop-level $\tan\beta$'s be close to each other in the large ζ regime.

At the tree-level, for small ζ, one expects a relatively large mixing angle as the expected cancellation in Δ^2 does not occur. At the loop-level, however, due to the reduced $\tan\beta$ one expects a smaller $Z - Z'$ mixing angle as can be seen from the form of Δ^2 in (14). Altough in the large ζ limit radiative correction to $\tan\beta$ is diminished, due to the increase in v_s ($-m_S^2$ increases) the loop-level $Z - Z'$ mixing angle will be still smaller than the tree-level one.

The lightest CP-even Higgs mass has the tree-level bound of

$$m_{h_1}^{2\,max} = M_Z^2 \cos^2 2\beta + (v_1^2 + v_2^2)[\frac{h_s^2 \sin^2 2\beta}{2} + g_{Y'}^2 (Q_1' \cos^2\beta + Q_2' \sin^2\beta)] \, . \tag{34}$$

Here the first term is the MSSM tree level bound, the h_s^2 term is the NMSSM contribution ($g_{Y'} = 0$ case), and finally the last term is the D-term contribution of $U(1)_{Y'}$ group. Using

the same approximations that had lead us to (32), a straightforward calculation yields the following one-loop bound:

$$\hat{m}_{h_1}^{2\,max} = m_{h_1}^{2\,max} + \beta_{h_t}[(\mu_s \cos\beta + A_t \sin\beta)^2 + 4S_{t\tilde{t}} m_t^2] \; . \tag{35}$$

As we observe from this equation, one-loop bound is always larger than the tree-level one. Since A_s^0 dependence of A_t is weak, the main contribution to the bound comes from m_t and μ_s terms, and it is maximized either by top-stop splitting contribution, or by the μ_s contribution. In fact, due to this μ_s dependence it will be much larger in $Heavy\ Z'\ Minimum$ than in $Light\ Z'\ Minimum$. In the parameter space we shall trace one expects the one-loop bound be dominated by m_t and μ_s terms in the small and large ζ regimes, respectively.

Had we included the entire particle spectrum and worked to all orders our results would be Q^2 independent. The one-loop expressions for $\hat{A}_s$ and $\hat{m}_2^2$ in (32) are actually Q^2 dependent and their dependence can be recovered by letting $S_{t\tilde{t}} \longrightarrow S_{t\tilde{t}} + \ln\frac{m_t^2}{Q^2}$. Therefore, if for some choice of Q^2, $\ln\frac{m_t^2}{Q^2}$ happens to be important, one can analyze these two quantities by intoducing the splitting function $S_{Q\tilde{t}} = \ln\frac{m_{\tilde{t}_1} m_{\tilde{t}_2}}{Q^2}$. Similarly, in the expression for $\tan\beta$, except for m_t^2 term, one can make the replacement $S_{t\tilde{t}} \longrightarrow S_{Q\tilde{t}}$ to take into account its Q^2 dependence. Unlike these, $\hat{\lambda}_2$ in (32), and lightest Higgs mass bound in (35) are independent of Q^2, so they exhibit the same behaviour for all Q^2. In general, all scalar mass-squared matrices are Q^2 dependent, but the lightest CP-even Higgs mass bound turns out to be scale independent. In the RGE analysis assumed that the scale of the SUSY breaking M_{SUSY} is around the weak scale, so the choice of $Q^2 \sim (v_1^2 + v_2^2)$ is necessary for consistency of the analysis. Thus, we do not expect the Q^2 dependence of the parameters to change the above-mentioned predictions significantly.

Until now we have based our analysis on the approximate formulae which were obtained by assuming that the top-stop splitting, $\ln\frac{m_t^2}{Q^2}$, and all gauge couping dependent terms are negligably small. These assumptions do not necessarily hold in the entire ζ spectrum, and thus it is needed to have a detailed picture for the ζ dependence of all these quantities.

IV. NUMERICAL ANALYSIS

In this section we shall investigate the effects of the radiative corrections on various quantities by an exact treatment of the problem using numerical techniques. To obtain the scalar mass matrices one has to calculate $\frac{\partial^2 V_1}{\partial\phi_i \partial\phi_j}$ evaluated at the VEV's. During the minimization we shall rescale all fields and parameters of mass dimension by A_t^0; consequently the parameters of the potential depend on a single quantity, ζ defined in (26). After minimizing the dimensionless potential, we recover the physical shell by requiring

$$A_t^0 = v/\sqrt{f_1^2 + f_2^2} \tag{36}$$

where $v = 246\ GeV$ is the Fermi scale. As we have already discussed in obtaining (16), this rescaling procedure works very well for the tree level potential [12] due to the uniqueness of the mass scale. However, radiative corrections do necessarily introduce an additional mass

scale Q^2. Thus, the rescaling invariance of the tree-level potential does not hold at the loop level. Using (36), one would rescale the basic log in (28) as

$$\ln \frac{\mathcal{M}^2}{Q^2} = \ln \tilde{\mathcal{M}}^2 \frac{A_t^{0\,2}}{Q^2} \tag{37}$$

which clearly requires the knowledge of A_t^0 which itself is something we aim to find. The determination of A_t^0 thus requires a consistency analysis where one inserts a trial value in this rescaled log, and compare it with the resulting one after the minimization. This procedure goes on until trial and output values for A_t^0 do match. We have done this numerically, and the result is shown in Fig.1 as a function of ζ.

In the analysis below we shall present tree-level and one-loop quantities on the same graph for the sake of easy comparison. In each graph the free variable is ζ, the ratio of Higgs trilinear coupling to top trilinear coupling at the SUGRA level. The starting value of ζ is chosen to be that one for which none of the VEV's vanish. On the other hand, the maximum of ζ is determined by its threshold value at which $m_{\tilde{t}_2}^2$ turns to negative due to large v_s values. This threshold shows up before squark soft masses turn to negative; so there is no danger of charge and/or color breaking in the range of ζ values we shall consider below.

Fig.1 shows the ζ dependence of A_t^0 for tree- and loop-level analyses. While tree-level A_t^0 peaks around $\zeta = 7$ with a value 73 GeV, one-loop A_t^0 peaks around $\zeta = 8$ hitting the value of 82 GeV. As the VEV's leave the small ζ regime (or f_2 dominated regime), the sum $f_1^2 + f_2^2$ approach its minimum, as f_1 and f_2 are driven to close enough values by A_s. That A_t^0 will be maximized around these ζ values follows from (36). After passing by this maximization point, all of the mass parameters become proportional to the associated power of ζ, as dictated by (25). Hence, in this 'large ζ' regime, we expect dimensionless doublet VEV's be approximately proportional to ζ because of which we observe an approximate $1/\zeta$ fall off in Fig.1. This kind of behaviour in A_t^0 reflects itself in all the relevant masses we shall discuss below. In solving the RGE's we have used the prescription $M_{1/2} = A_t^0$, which implies the weak scale masses of $\sim 2.6 \times A_t^0$, $0.8 \times A_t^0$, $A_t^0/4$, and $A_t^0/10$ for $SU(3)_c$, $SU(2)$, $U(1)_Y$, and $U(1)_{Y'}$ gauginos, respectively. Thus, depending on the present and future experimental limits on the gaugino masses of different group factors, one can restrict ζ to a certain range of values, keeping in mind that the choice $M_{1/2} = A_t^0$ itself is not necessarily unique.

We plot the ζ dependence of $\tan\beta$ in Fig. 2. As we observe from this figure, for small ζ values, loop contributions do really push $\tan\beta$ to smaller values. Again in agreement with our expectations, for large ζ, both the tree level and loop results come closer rapidly, and gradually approach to unity . The difference between one-loop and tree-level $\tan\beta$'s fall below 1% after $\zeta \sim 8$.

In Fig.3 we present the ζ dependence of the $Z - Z'$ mixing angle α. In agreement with the predictions of the last section, one-loop mixing angle is smaller than the tree level one everywhere. As we see from this figure, the phenomenological bound of $\alpha_{max} \sim a\ few \times 10^{-3}$ after $\zeta \sim 7$ is comfortably satisfied after $\zeta \sim 7$. The last point about this figure is that for large ζ values one-loop and tree-level results remain approximately parallel, indicating the fact that both doublet VEV's reach their limiting values controlled by A_s, and SM-singlet VEV enter the $-m_S^2$ dominated regime.

Another important quantity, M_{Z_2}, is shown in Fig. 4 as a function of ζ. First, we see that loop corrections generally increase the Z_2 mass in the entire ζ range. Both tree-level and

one-loop masses increase until $\zeta \sim 10$ in accordance with A_t^0 in Fig.1. Likewise, in parallel with the behaviour of A_t^0 M_{Z_2} decreases gradually after $\zeta \sim 10$, and is expected to saturate after some point due to the fact that ζ dependence of A_t^0 and dimensionless SM-singlet VEV are almost inversely proportional to each other in this range of ζ values. The one-loop M_{Z_2} peaks at $\zeta \sim 11$ by taking the value of $\sim 405\, GeV$; thus, it cannot increase indefinitely with ζ. As expected, the tree-level M_{Z_2}, in similarity with the tree-level A_t^0, peaks at $\zeta \sim 10$, with a value $\sim 330\ GeV$. The values taken by M_{Z_2} depends crucially on the value of $g_{Y'}$. Under the normalization in (8), and the $U(1)_{Y'}$ charge assignments in (9), the solution of the RGE's yield $g_{Y'}/g_Y \approx 0.65$ at the weak scale. This ratio would push the value of M_{Z_2} above $600\, GeV$, if $g_{Y'} = g_Y$ were the case. One notes that the recent Tevatron result [18] giving $M_{Z_2} \geq 590\, GeV$ would be well satisfied if $g_{Y'}$ were equal to g_Y.

As explained in the Introduction, one of the basic aims of constructing such extended models is of course the dynamical formation of the MSSM μ parameter. The effective μ parameter in the present model has the ζ dependence shown in Fig. 5, for which we have almost the same behaviour observed in Z_2 mass, as both are controlled by A_t^0. The one-loop μ_s peaks around $\zeta = 11$, and takes the value $\sim 350\, GeV$ at this point. Similarly, the tree level μ_s peaks around $\zeta = 10$ with a value $\sim 280\ GeV$.

Finally, in Fig. 6, we present the ζ dependence of the lightest Higgs mass bound, $m_{h_1}^{max}$, which is seen to satisfy the predictions of the last section. As we see from (34), the tree level bound depends solely on the doublet VEV's, so that after reaching the $\tan\beta \sim 1$ regime the bound is maximized and saturated at $m_{h_1}^{max} \sim 118\, GeV$. In the same way until leaving the small ζ region, one-loop bound also increases and hits the value $\sim 125\, GeV$ in the far end of the total ζ range. The fact that one-loop bound saturates much later than the tree-level one is due to the μ_s dependence of the radiative corrections.

V. CONCLUSIONS AND DISCUSSIONS

In this work we have investigated one-loop contributions to certain low-energy quantities in the framework of the effective potential approach, using an RGE-improved radiatively corrected scalar potential, following from the superpotential in (1). However, derivation of the entire low-energy particle spectrum (such as top, bottom, and τ masses) requires the study of a more general superpotential involving, in addition to the superpotential in (1), exotics predicted in most string models and non-renormalizable quartic mass terms from which light fermion masses follow [16,19]. Here we have restricted ourselves mainly to the study of certain low-energy quantities determined by the Higgs sector of the model, for which the typical superpotential in (1) should suffice [12,19].

Among the low-energy quantities we have worked out, Z' boson and lightest Higgs mass bound are of phenomenological importance. The search for Z' [20] will be one of the goals of the next generation accelerators. In near future, LEP II will be searching for Z' boson in leptonic and WW channels. Besides this, LHC will search for Z' boson with quark-antiquark fusion processes. In general, the exclusion limits of Z' mass and its couplings depend on the model and collider parameters [21]. The $U(1)_{Y'}$ charges of the present model are generation dependent, and thus, the constraints on its Z' boson is weaker than that of the generation independent ones. The $Z - Z'$ mixing angle (See Fig. 3) is small enough to supress the effects

of Z' fermion couplings in the Z -pole observables [22]. The Z' mass in the present model has an upper bound of $\sim 400\,GeV$, and satisfies the presently existing phenomenological bounds.

The lightest Higgs mass bound turns out to be $\sim 125\,GeV$ [23] in MSSM. In NMSSM, however, it is $\sim 140\,GeV$ [10]. In the present model, it turns out to be $\sim 125\,GeV$. The bounds of the present model and MSSM practically coincide, however, the bound in the present model is expected to increase slightly if the NNL corrections are taken into account [23]. In near future, the lightest Higgs boson will be discovered at LEP II if $m_{h_1} \leq 95\,GeV$, and at FNAL in $m_{h_1} \leq 120\,GeV$ after accumulating an integrated limunosity of 25-30 fb^{-1} [24].

In conclusion, we have analyzed the efects of the radiative corrections on the various low energy quantities in the present model by taking the contributions of top and stops into account. As we have shown graphically, the one-loop improvment in the low energy parameters are no way negligable. Moreover, the one-loop corrections support the satisfaction of the phenomenological requirements compared to the bare tree-level potential. The findings of the work will be tested in the near-future colliders.

VI. ACKNOWLEDGEMENTS

One of us (D. A. D.) thanks Paul Langacker for his helpful remarks at the earliest stages of this work.

REFERENCES

[1] M. Cvetic, P. Langacker, Phys. Rev. D54 (1996) 3570.
[2] G. F. Giudice, A. Masiero, Phys. Lett. B206 (1988) 480.
[3] H. P. Nilles, Phys. Rep. 110 (1984) 1.
[4] S. K. Soni, H. A. Weldon, Phys. Lett. B126 (1983) 215.
[5] A. Brignole, L. E. Ibanez, C. Munoz, C. Scheich, Z. Phys. C74 (1997) 157 ; H. B. Kim, C. Munoz, Mod. Phys. Lett. A12 (1997) 315; A. Brignole, L. E. Ibanez, C. Munoz, hep-ph/9707209.
[6] D. Matalliotakis, H. P. Nilles, Nucl. Phys. B435 (1995) 115.
[7] W. Hollik, hep-ph/9703231.
[8] M. Carena, M. Quiros, C. E. M. Wagner, Nucl. Phys. B461 (1996) 407
[9] M. Quiros, hep-ph/9703412.
[10] T. Elliot, S.F. King, P.L. White, Phys. Lett. B314 (1993) 56; U. Ellwanger, Phys. Lett. B303 (1993) 271.
[11] P. Langacker, hep-ph/9411247.
[12] M. Cvetic, D. A. Demir, J. R.Espinosa, L. Everett, P. Langacker, Phys. Rev. D56 (1997) 2861.
[13] P. Langacker, N. Polonsky, Phys. Rev. D52 (1995) 3081.
[14] V. S. Kaplunovsky, Nucl. Phys. B307 (1988) 145.
[15] H. E. Haber, M. Sher, Phys. Rev. D35 (1987) 2206.
[16] A. E. Faraggi, Phys. Lett. B274 (1992) 47, *ibid.*, B377 (1996) 43.
[17] J. Ellis, J. F. Gunion, H. E. Haber, L. Roszkowski, F. Zwirner, Phys. Rev. D39 (1989) 844.
[18] F. Abe et. al., CDF Collab., Phys. Rev. Lett. 79(1997)2192.
[19] J. R. Espinosa, hep-ph/9707541.
[20] J. Hewett, T. Rizzo, Phys. Rep. 183 (1989) 193.
[21] S. Riemann, hep-ph/9710564; A. Leike, hep-ph/9708436; T. G. Rizzo, hep-ph/9710229
[22] K. S. Babu, C. Kolda, J. March-Russel, hep-ph/9710441
[23] J. A. Casas, J. R. Espinosa, M. Quiros, A. Riotto, Nucl. Phys. B167 (1995) 3.
[24] S. Stange, W. Marciano, S. Willenbrook, Phys. Rev. D49 (1994) 1354.

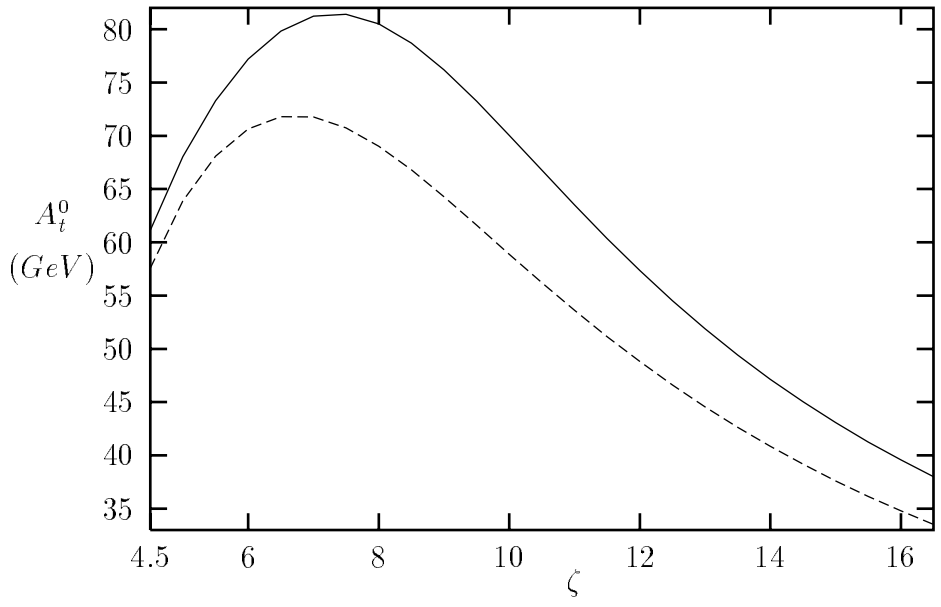

Figure 1: Dependence of A_t^0 on ζ (solid line: one-loop, dashed line: tree-level)

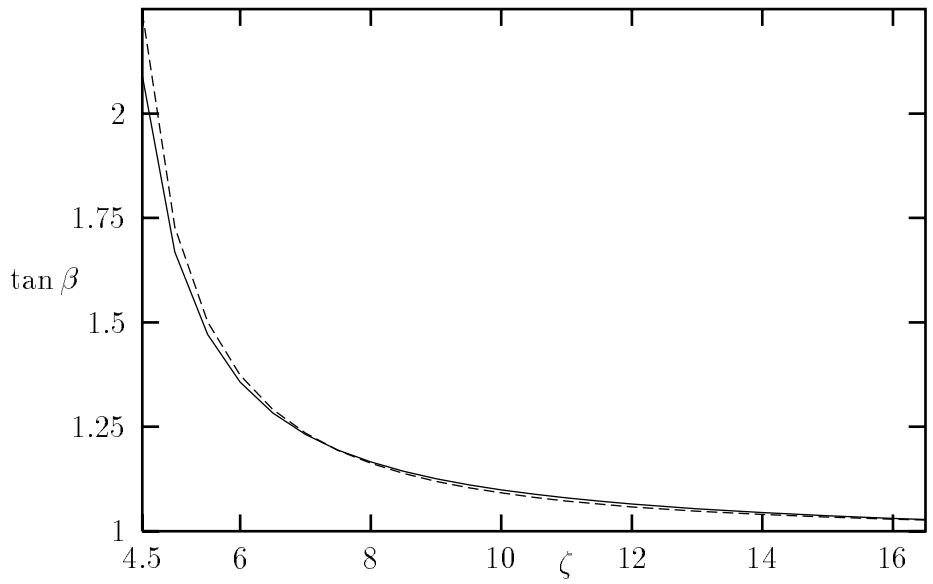

Figure 2: Dependence of $\tan\beta$ on ζ (solid line: one-loop, dashed line: tree-level)

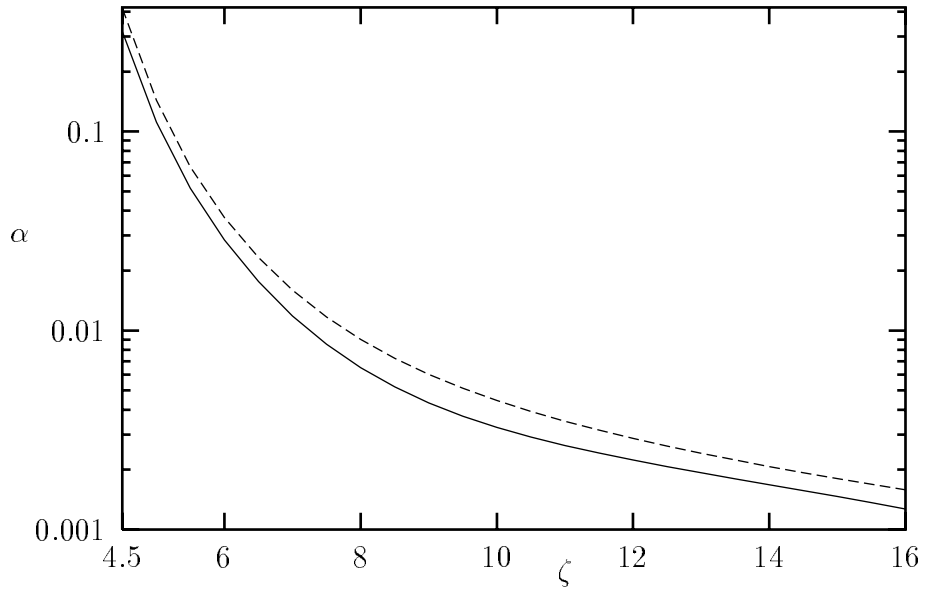

Figure 3: Dependence of α on ζ (solid line: one-loop, dashed line: tree-level)

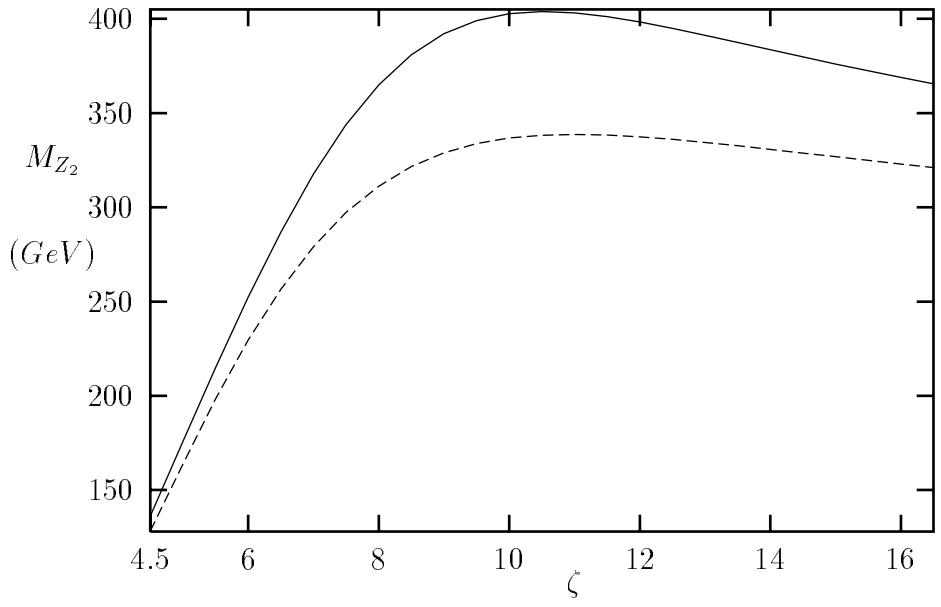

Figure 4: Dependence of M_{Z_2} on ζ (solid line: one-loop, dashed line: tree-level)

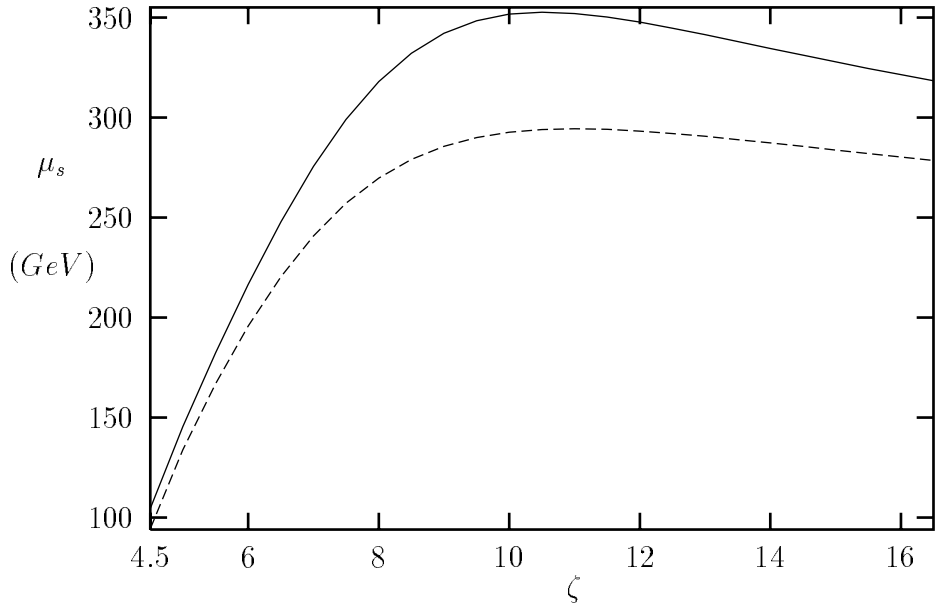

Figure 5: Dependence of μ_s on ζ (solid line: one-loop, dashed line: tree-level)

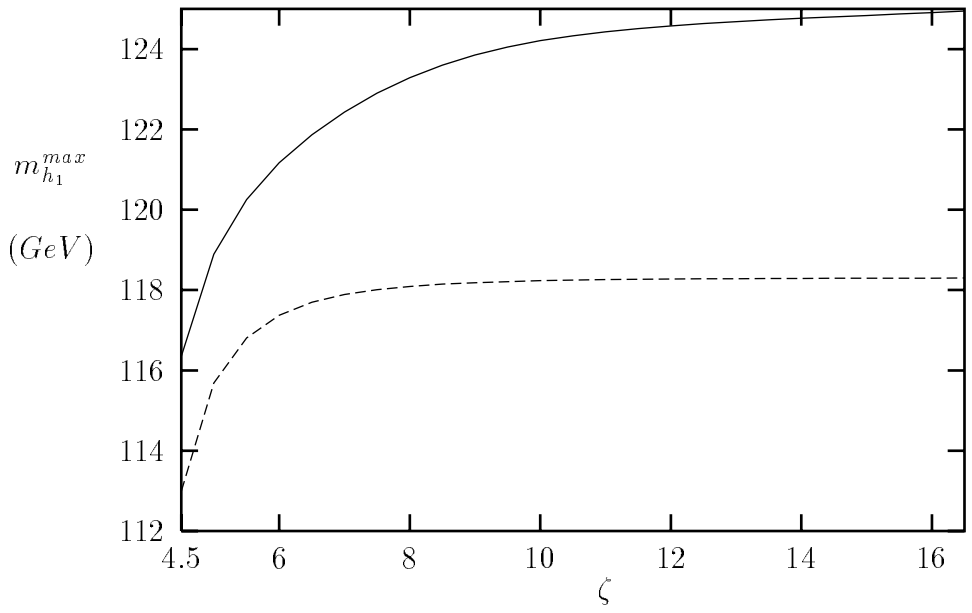

Figure 6: Dependence of $m_{h_1}^{max}$ on ζ (solid line: one-loop, dashed line: tree-level)